DESIGN AND EXPERIMENTAL RESEARCH OF A PORTABLE WALNUT HARVESTER BASED ON ELECTROMAGNETIC EXCITATION TECHNOLOGY

/

基于电磁激励技术的便携式核桃采摘机设计与试验研究

Na JIA[1)] Guangqiu LI[1)] Anguo HU[2)] Qin CHEN[*3)]

[1)] Northeast Forestry University, College of Mechanical and Electrical Engineering/ China;

[2)] Yongkang Weili Technology Co, Ltd / China

[*3)] The Yunnan Provincial Academy of Forestry and Grassland Sciences YangBi Walnut Research Institute/ China;

Tel: +86 18686870636; E-mail: 876765338@qq.com

Corresponding author: Qin Chen

DOI: https://doi.org/10.35633/inmateh-74-30

Keywords: *Electromagnetic excitation technology, Walnut harvesting machine, Portable machinery, Agricultural mechanization, Parameter optimization*

ABSTRACT

With the development of agricultural mechanization and the expansion of fruit tree cultivation, effective harvesting techniques have become crucial for boosting yield and reducing labor costs. This is particularly true in hilly areas with complex terrains where traditional, large-scale harvesting machinery struggles to be effective. This study designed and experimentally validated a portable walnut harvester based on electromagnetic excitation technology, aiming to enhance harvesting efficiency and reduce labor intensity in these areas. The harvester integrates electromagnetic excitation technology with the design of a lightweight, handheld electric cart, optimizing the machine's adaptability and operational flexibility across various terrains. Through field testing, the vibration effects of the machine under different branch diameters and impact locations were evaluated, and the impact parameters were optimized using Design-Expert software. Experimental results indicate that the machine can operate effectively at maximum pitch angles while delivering powerful impact forces to harvest walnuts efficiently. Furthermore, by optimizing the vibration frequency and impact location for branches of different diameters, recommended parameters for using the equipment were provided. This study not only demonstrates the potential application of electromagnetic excitation technology in agricultural machinery but also offers a viable mechanized solution for orchards in similarly complex terrains.

摘要

随着农业机械化的发展和果树种植业的扩展，有效的采摘技术成为提升产量和降低劳动成本的关键。尤其在地形复杂的丘陵地区，传统的大型采摘机械难以发挥效用。本研究设计并实验验证了一种基于电磁激励技术的便携式核桃采摘机，旨在提高这些地区的采摘效率并减轻劳动强度。该采摘机结合了电磁激励技术和轻便的手扶式电动推车设计，优化了机械在不同地形下的适应能力和操作灵活性。通过实地测试，我们评估了机器在不同枝杆直径和撞击位置下的激振效果，并采用 Design-Expert 软件进行了撞击参数的优化。实验结果表明，该机械能在最大俯仰角度下有效操作，同时提供强大的撞击力，有效地采摘核桃。此外，通过对不同直径枝杆的激振频率和撞击位置的优化，提供了设备使用的推荐参数。该研究不仅展示了电磁激励技术在农业机械中的应用潜力，也为类似地形复杂的果园提供了一种可行的机械化解决方案。

INTRODUCTION

As global populations continue to rise and advancements in agricultural mechanization progress, efficient crop harvesting technologies are becoming increasingly vital. Walnuts, a fruit of significant economic value, are extensively cultivated in various provinces in China such as Yunnan, Xinjiang, and Sichuan (*Wei Li, 2023; Jia Meng et al., 2023*). Particularly in Yunnan Province, walnut cultivation leads the nation with an area of 286.87 thousand hectares and a production of 1.48 million tons (*Honghong Yu et al., 2019*). Due to the distinct seasonality of walnut harvesting, delays in harvesting can directly impact the quality of the walnuts and result in substantial economic losses. Consequently, enhancing the efficiency of walnut harvesting has been a focal point in forestry and fruit industry research.

In recent years, as the level of agricultural mechanization has improved, the development and application of large-scale vibratory harvesting machines have achieved notable success. For instance, in 2017, *Hoshyarmanesh et al.* designed a vibratory olive harvester, identifying the optimal excitation frequency for olive trees at 20Hz (*Hoshyarmanesh et al., 2017*). Castro-Garcia S developed a vibratory harvester for citrus fruits, determining through simulations and experiments that the resonance range for different maturities of citrus lies between 4.5 to 5Hz (*Castro-Garcia S et al., 2017*). In 2019, Zicheng Gao developed a suspended vibratory camellia fruit harvester, using dual eccentric blocks as the source of vibration and a tracked chassis for mobility. Their trials indicated that the acceleration of camellia fruit tree branches varied cyclically with vibration, with the vibratory frequency and clamping height significantly affecting trunk amplitude, and fruit drop rate correlating positively with harvesting frequency and inversely with clamping height. At a frequency of 15Hz and a clamping height of 1300mm, the fruit drop rate and flower drop rate reached 95.1% and 4.8%, respectively (*Zicheng Gao et al., 2019*). In 2022, Xiaoqiang Du designed a tracked tea oil fruit vibratory harvester, employing a crank rocker to drive multiple rows of tapping rods, achieving a fruit harvesting rate of 87.56% and a bud drop rate of 25.86% at 360r/min hydraulic motor operation (*Xiaoqiang Du et al., 2022*). In 2023, Shuqi Shang designed an apple vibratory harvester using eccentric blocks as the source of vibration, towed by a tractor. At a vibration frequency of 10Hz, an amplitude of 1.6cm, and a clamping height of 58.7cm, the fruit detachment rate reached 95.9% with a fruit damage rate of only 1.3% (*Shuqi Shang et al., 2023*).

Although large-scale vibratory harvesting machines have shown significant effectiveness in improving the efficiency of orchard fruit harvesting, their application in mountainous and hilly areas still poses major challenges. These machines typically rely on eccentric blocks to generate the necessary vibratory force, leading to an increase in overall weight, which restricts mobility and operability. In areas with complex terrain and steep slopes, the operational safety and flexibility of these devices are substantially reduced, and the high cost of the equipment further limits their widespread use in these regions (*Wenting Jin et al., 2023*).

Given the challenges posed by complex terrains, the development of portable walnut harvesting equipment becomes crucial. In 2018, Chengmao Cao designed a portable walnut harvester that mimics human-like high-altitude beating actions using an eccentric wheel and a driven pendulum piece. Although experimental data indicated that this device exhibited a higher picking cleanliness, the small impact area per beat resulted in lower harvesting efficiency, and prolonged manual operation increased the labor intensity for workers (*Chengmao Cao et al., 2018*). Subsequently, in 2021, Zensong Li developed an integrated manual and automatic walnut harvester. Experiments demonstrated that at excitation frequencies of 16-18 Hz, the machine achieved average picking rates of 83.9%-88.0%. However, increased excitation amplitude and duration led to greater damage to branches and shoots (*Zensong Li et al., 2021*). In 2023, Huibin Zhu and Zhang Wenkai designed a gasoline-powered walnut harvesting machine, which exhibited an optimal picking cleanliness of 86.5% in simulation tests. Nevertheless, due to limitations in the design of the clamping points, its cleanliness could not be further improved, highlighting the necessity to consider more adjustable clamping points in the design to optimize performance (*Huibin Zhu et al., 2023*).

These studies indicate that despite some progress in addressing walnut harvesting challenges in mountainous and hilly regions through portable harvesting equipment, the design reliance on eccentric masses as excitation sources continues to restrict the portability and ease of operation of these devices. Electromagnetic excitation technology, as an innovative solution, demonstrates significant advantages due to its simple structure, light weight, strong and controllable excitation force. This technology not only effectively reduces the equipment weight but also allows for the adjustment of excitation frequency to flexibly meet the harvesting needs of different tree species and fruits, greatly enhancing the practicality and application range of portable walnut harvesting devices.

MATERIALS AND METHODS

System Overview and Operating Principle

System Components

The overall structure of the portable walnut harvester based on electromagnetic excitation technology includes the following main components: an impact clamping device (comprising an impact device and a clamping device), a control rod, an adjustable support column, Hanging Connector, an electric dual-wheel handcart, and associated motor and electromagnetic control devices. The schematic of this structure is detailed in Fig. 1.

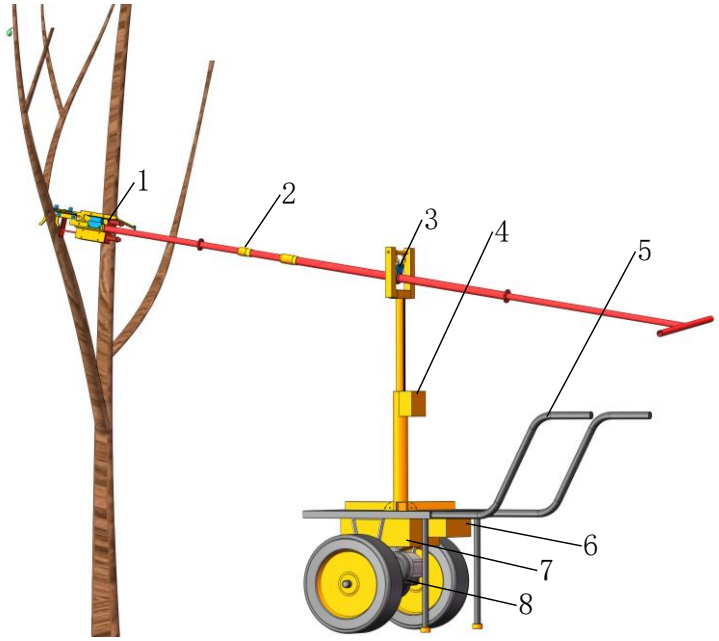

Fig. 1 - Schematic Diagram of Walnut Harvester Structure

1.Impact Clamping Device; 2. Control Rod; 3. Hanging Connector; 4. Adjustable Support Column; 5. Electric dual-wheel handcart; 6. Control Box; 7. Power Storage Compartment; 8. 0.8kW Motor

The impact clamping device consists of a clamping device and an impact device, both fixed to the control rod via a convex connecting plate. The clamping device utilizes a pre-tensioned spring to achieve a clamping gap corresponding to the varying thicknesses of branches, which is then locked by the magnetic force of a rectangular solenoid.

This design allows the clamping device to adaptively grip branches of different thicknesses using the self-weight of the impact clamping device. The exciting electromagnet provides an effective impact force, enabling efficient excitation of the branches. The control rod is suspended from the head of the adjustable support column via a chain, significantly reducing the transfer of vibrational forces to the operator during excitation, thereby enhancing operational comfort.

The adjustable support column is connected to the Electric dual-wheel handcart through bolts, allowing operators to quickly switch between targets during the harvesting process. The Electric dual-wheel handcart is equipped with a differential to drive both wheels, with a motor power of 0.8 kW and a maximum climbing angle of 40°, sufficient to meet the mobility and on-the-spot turning requirements of the harvester in hilly areas. The motor control device of the Electric dual-wheel handcart and the control device for the exciting electromagnet are both housed within a control box, sharing a power source to simplify system configuration and operation.

Before initiating the harvesting operation, operators must first adjust the Electric dual-wheel handcart to ensure it maintains an appropriate distance from the main trunk of the walnut tree. This process involves adjusting the position of the Electric dual-wheel handcart and its telescopic section, as well as the height of the adjustable support column based on the distribution height of the branches, thus optimizing the ergonomics of the operation and enhancing harvesting efficiency.

The operator controls the control rod to position the clamping device above the target branch. Subsequently, the operator reduces the force applied at the handle of the operation section, allowing the impact clamping device to naturally fall and engage the branch into the working interval of the clamping device. Under the tension provided by the pre-tensioned spring, the clamping device automatically adapts to branches of different thicknesses, ensuring the stability of subsequent clamping operations. Once positioned, the air switch is activated, energizing the rectangular solenoid, which then locks the clamping gap formed to match the diameter of the clamped branch, completing the clamping process.

Following this, the switch of the exciting electromagnet controller is triggered. According to the preset operating frequency of the control system chip, the exciting electromagnet drives the push plate to impact the clamped branch. The impact of the push plate accelerates the fruit at the end of the branch; when the inertial force exerted on the fruit exceeds the binding force of the fruit stem, the fruit detaches from the branch, completing the harvesting process.

Design of Key Components

Design of the Control Rod Structure

The control rod is a critical component of the portable walnut harvester, directly impacting the equipment's operational flexibility and efficiency. In this design, the control rod consists of several functional parts, including the connection segment, control segment, telescopic segment, Rotating Clamp Head, and Hanging Connector, with the detailed structure presented in Fig. 2. The design of the control rod focuses on enhancing the ergonomic adaptability of operations and reducing physical labor intensity.

The Hanging Connector on the control rod are linked to the adjustable support column via a chain, allowing the control rod to be suspended in mid-air, effectively reducing the reactive forces transmitted to the operator's hands during the excitation process. In terms of connections, the control segment, connection segment, and telescopic segment utilize flange connections, which allow for rapid disassembly and assembly through hand-tightened nuts, greatly increasing the efficiency of equipment maintenance and adjustment.

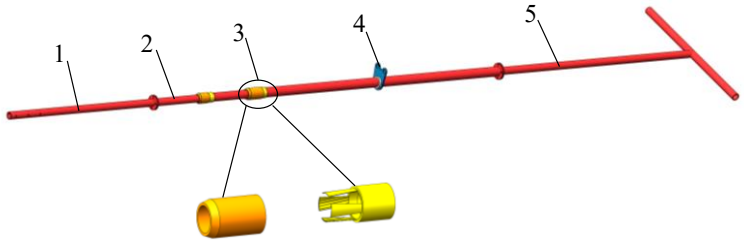

Fig. 2 - Schematic Diagram of the Control Rod Structure

1. Connection Segment; 2. Telescoping segment; 3. Rotating Clamp Head; 4. Hanging Connector; 5. Control Segment

The control rod is made from stainless steel hollow tubes, designed to reduce overall weight and enhance structural corrosion resistance, adapting to various field environments. The telescopic segment is designed as a combination of three stainless steel tubes of different thicknesses and lengths, connected by a Rotating Clamp Head, allowing for rapid adjustment of the control rod length to accommodate different operator habits and work environments. The adjustable range of the control rod length is from 1.3 to 2.6 meters, meeting the needs from low to high work requirements, and the longest rod segment does not exceed 1.3 meters when disassembled, facilitating transportation and storage.

The flexible suspension of the telescopic segment allows the control rod to rotate or swing circumferentially on the adjustable support column via Hanging Connector, accommodating branches growing at various angles. Based on ergonomic design, the operator's hand-holding position is maintained at a height of 0.8 to 1.2 meters to optimize the operating experience and efficiency. The support panel height of the Electric dual-wheel handcart is 0.6 meters, which, in conjunction with the adjustment of the control rod, can meet different harvesting height requirements.

Taking practical harvesting heights of 3.2 meters and 0.9 meters as examples, the angle between the control rod and the horizontal plane as well as the lifting range of the adjustable support column were precisely calculated using formulas (Formulas 1-4), ensuring the accuracy and safety of the operation.

$$\sin\theta = \frac{l}{H - h_1} \text{ [°]} \quad (1)$$

where: l - length of the control rod, [m]; H - actual harvesting height, [m]; h_1 - height of the control rod grip, [m]; θ - Pitch angle of the control rod, [°].

Using equation (2) to calculate the pitch angle of the control rod, the height of the fixed position of the Hanging Connector is determined:

$$\theta = \arcsin\frac{l}{H - h_1} \text{ [°]} \quad (2)$$

$$h = \tan\theta(l_1 - h_2) \text{ [m]} \quad (3)$$

$$h = \tan\left(\arcsin\frac{l}{H - h}(l_1 - h_2)\right) \text{ [m]} \quad (4)$$

where: l_1 - horizontal distance between the control rod grip and the adjustable support column, [m]; h_2 -height of the Electric dual-wheel handcart panel, [m]; h - height of the adjustable support column 's head, [m].

The calculations indicate that the optimal fixed position for the Hanging Connector on the control rod should be at 1.3 m, while the lifting range of the adjustable support column should be set between 0.6 and 1.2 m to accommodate different working conditions. Under these settings, the pitch angles of the control rod will be 12.68° and 31.26°, respectively, ensuring optimal ergonomics and operator comfort during operation.

Design and Development of the Impact Clamping Device

The impact clamping device is a core component, consisting of parts such as the push plate, exciting electromagnet, convex connecting plate, and clamping mechanism (including the clamping head, pre-tensioned spring, slide rail, and rectangular solenoid), with the specific structure shown in Fig 3. Both the exciting electromagnet and the rectangular solenoid, along with the clamping head, are bolted onto the control rod. By clamping the branches, the weight of the impact clamping device and most of the reactive force during excitation are transferred to the branch, significantly reducing the labor intensity for workers engaged in prolonged operations. The two exciting electromagnets have the same model and are installed at the corresponding position on the convex connecting plate to ensure that the kinetic energy output of the exciting electromagnet to the pushing plate can be balanced during the excitation process. The dynamic clamping head is connected to the fixed clamping head via a slide rail and connected at the end to the pre-tensioned spring, facilitating adaptive clamping.

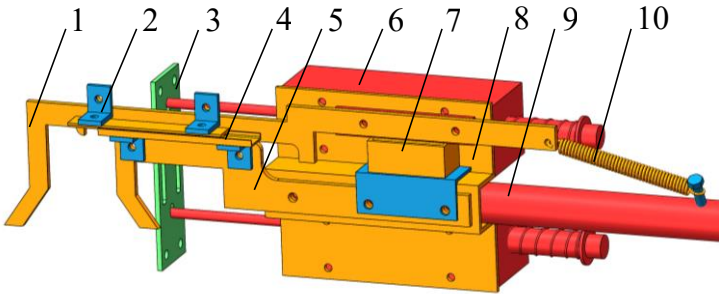

Fig. 3 - Schematic Diagram of the Impact Clamping Device Structure

1. Dynamic Clamp Head; 2. Angle Bracket; 3. Push Plate; 4. Slide Rail; 5. Fixed clamp head; 6. Exciting electromagnet; 7. Rectangular solenoid; 8. Convex Connection Plate; 9. Connection Segment; 10. Pre-tension Spring

Design and Development of the Impact Device

The key to the design of the impact device lies in ensuring the optimal ratio of kinetic energy to weight of the push plate, to maximize impact efficiency without compromising the stability and durability of the equipment. The impact clamping device operates in an upward-looking posture; thus, the exciting electromagnet needs to overcome the gravitational work of the push plate during excitation. Excessive weight of the push plate could significantly affect the excitation frequency and impact kinetic energy of the electromagnet, while too light a weight may lead to deformation of the push plate or insufficient impact energy. Therefore, to ensure that the impact device's kinetic energy meets the harvesting requirements, the weight and material properties of the push plate are especially crucial. Using NM450 material for the push plate, which has a yield strength exceeding 1100 MPa and impact resistance and wear resistance three times that of the commonly used Q235 material, enhances the impact performance and long-term durability of the entire device (*Yi Cao et al., 2023*).

Upon impact, walnut branches facilitate the accelerated motion of the fruit. According to tests on the separation force between walnut fruit and branches, the average separation force along the stem direction is 8N. As the direction of force application increasingly deviates from the fruit's growth direction, the required separation force decreases. Based on the average weight of mature walnuts, 60-80g, using formula (5), the necessary acceleration for walnut detachment is calculated to ensure that excitation at any angle can effectively harvest the fruit (*Tuqiang Chen et al., 2023; Chunshou Ye et al., 2022*).

$$F_f = m_h a_f \text{ [N]} \quad (5)$$

where: F_f - force required for fruit detachment, [N] ; m_h - weight of a single walnut, [g]; a_f - acceleration needed for fruit to detach from the branch, [m/s²].

During the harvesting process, when the walnut's acceleration reaches 100 m/s², effective harvesting can be achieved. As per equation (6), the magnitude of the electromagnetic force is influenced by factors including the length of the striking pin and the coil's excitation current. Therefore, based on this data, when selecting the model of the exciting electromagnet, it is advisable to choose a model with a long striking pin and high current to ensure optimal mechanical performance (*Mengkun Lu et al, 2023; Tong Huang et al., 2018*).

$$F_D = \frac{dW}{dx} = \frac{1}{2} i^2(t) \frac{\partial L(x)}{\partial x} \text{ [N]} \quad (6)$$

where: F_D - Electromagnetic force, [N]; W - Magnetic energy, [J]; $L(x)$ - Inductance value related to the position of the striking pin, [H]; $i(t)$ - Excitation current of the coil, [A].

Models with longer movable striking pin and greater current capabilities to enhance the impact strength and reliability of the equipment were preferred. The selected model of the exciting electromagnet is DC24 - 100mm, characterized by its compact size, lightweight, operating voltage of 24V, current of 8A, stroke of 100mm, and operating frequency set between 1 - 3.5 Hz. It provides a maximum impact force of over 50N, making it highly suitable for the needs of this project.

Optimization Experiments of the Impact Device

In this study, the performance evaluation of the excitation electromagnet was conducted by overcoming the gravity of the push plate. In order to further explore the impact force of the impact device under different postures, a series of impact tests was designed considering the influence of the design parameters of the picking machine. Acceleration sensors were pasted on the surface of the push plate to collect experimental data (*Hou, Junming, et al., 2024*). Two different weights (100g and 600g) of push plates were used, and four experiments were conducted at elevation angles of 0°, 10°, 20° and 30°, with four groups in each experiment. Each group lasted for 4s, and the duration of each group was divided into five equal parts, taking the average value as the numerical value of that stage. The specific experimental setup is shown in Figure 4, and the experimental results are shown in Figure 5.

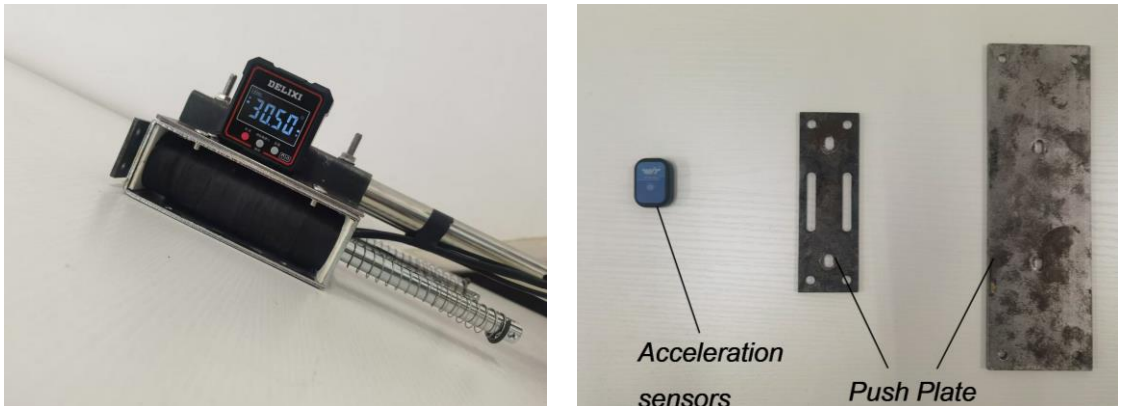

Fig. 4 - Device for Impact Testing

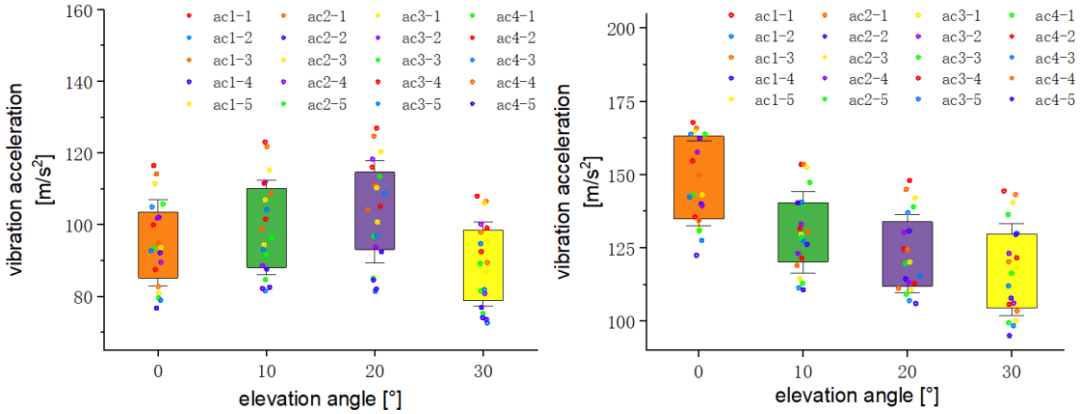

a. 100g Push Plate b. 600g Push Plate

Fig. 5 - Performance Testing of the Impact Device

As shown in Fig 6a, the 100g push plate recorded a maximum acceleration of 118 m/s² at a 0° tilt angle, while a peak acceleration of 128 m/s² was observed at a 20° tilt angle, indicating an initial increase and subsequent decrease in acceleration with increasing tilt angle. Furthermore, the operating frequency of the push plate had a minimal impact on the test results.

The iron core was measured to weigh 437g, and based on formula (16), the maximum instantaneous impact force of the 100g push plate under peak acceleration was calculated to be 68.75N. This calculation provides a direct quantification of the impact performance of the impact device.

$$F_s = (m_2 + m_3)\ a \quad [\text{N}] \tag{16}$$

where: F_S - the impact force measured by the impact device, [N]; m_2 - mass of the striking pin, [m]; m_3 - mass of the push plate, [m]; a- acceleration recorded, [m/s^2].

For the 600g push plate, Fig. 6b shows that the highest acceleration recorded was 170 m/s² at a 0° tilt angle, with a decreasing trend in acceleration as the tilt angle increased, reaching 151 m/s² at 30°. Unlike the 100g push plate, the 600g push plate significantly impacts the operating frequency of the impact device.

Accordingly, the instantaneous impact force for the 600g push plate at maximum acceleration was calculated to be 176N. This result highlights the significant increase in impact force due to increased weight and also points to the influence of weight on the overall operating frequency of the device.

In this study, a detailed analysis of the effects of tilt angle and push plate mass on the performance of the impact device was conducted. Experimental results indicate that the mass of the push plate and the tilt angle are important factors affecting the impact force. Specifically, when the mass of the push plate is low, the impact force initially increases and then decreases with increasing tilt angle. This phenomenon can be explained by changes in the efficiency of kinetic energy transfer at different angles: an initial increase in tilt may facilitate more effective energy transfer, while at higher tilt angles, impact efficiency begins to decrease due to mechanical structural limitations.

Conversely, for heavier push plates, increasing the tilt angle leads to a gradual decrease in impact force. This is mainly because the increased weight leads to greater kinetic energy loss during transfer, especially at larger tilt angles. Additionally, the mass of the push plate significantly affects the operating frequency of the exciting electromagnet, requiring the electromagnet to operate at lower frequencies to maintain sufficient impact force for heavier push plates.

Therefore, when selecting a push plate, it is essential to consider the combined effects of tilt angle and operating frequency of the electromagnet. This comprehensive consideration aims to optimize the overall performance of the impact device, ensuring optimal impact force under various working conditions. Table 1 lists detailed data on the impact forces under different configurations.

Table 1

Impact Force of the Impact Device

Elevation angle [°]	0	10	20	30
Impact force [N]	155-130	150-125	142-110	135-105

Design and Analysis of the Clamping Device

The clamping device achieves precise positioning of the branches to be clamped through the self-weight of the impact clamping device and the guide angle, and confirms the clamping gap relative to the diameter of the clamped branch using a pre-tensioned spring, ultimately utilizing the magnetic attraction principle of the Rectangular solenoid to lock the clamping gap formed around branches of varying thicknesses. Whether the clamping device can form and lock a corresponding clamping gap for branches of different thicknesses depends on the tension provided by the pre-tensioned spring and the magnetic force of the Rectangular solenoid. Therefore, an analysis and calculation of the forces during the clamping process are necessary, as shown in Fig. 6.

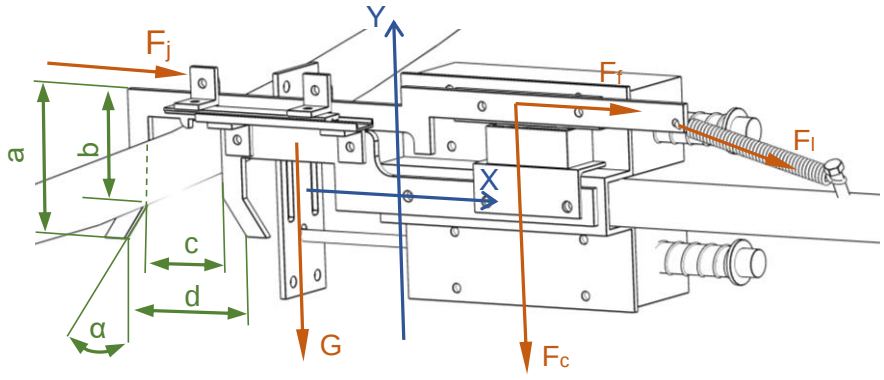

Fig. 6 - Force Analysis Diagram of the Clamping Device

Analyzing the forces in the coordinate system yields:

$$\begin{Bmatrix} F_y = F_l \sin\alpha + \mu F_N - nG\cos\alpha \\ F_x = F_l \cos\alpha + nG\sin\alpha \end{Bmatrix} \quad (7)$$

where: F_l - tension provided by the pre-tensioned spring, [N]; μ - coefficient of friction between the clamping device and the bark; n - ratio of the support force to gravity acting on the impact clamping device; G - gravity of the impact clamping device, [N]; α - deflection angle of the guide angle, [°];

If the clamping device is to adapt to branches of various thicknesses, it is required:

$$\begin{cases} F_y < 0 \\ F_x = -F_N \end{cases} \quad (8)$$

Combining and simplifying the above expressions, it is obtained:

$$F_l < \frac{\sin\alpha + \mu\cos\alpha}{nG(\cos\alpha - \mu\sin\alpha)} \text{ [N]} \quad (9)$$

For a cylindrical helical spring:

$$F_l = k \cdot \Delta x \text{ [N]} \quad (10)$$

where: k - spring stiffness coefficient, [N/m]; Δx - spring extension, [mm].

The clamping mechanism is self-adapting to a wide range of branch thicknesses, provided that the distance between the ends of the guide angles, d, is greater than the diameter of the largest clamped branch. The cross-sectional diameters of walnut tree branches mostly range from 30 to 90 mm, tapering from the main trunk to the end of the branch. Hence, the working range of the clamping h d >50 mm.

From this, the guide angle can be deduced:

$$\alpha = \arctan\frac{a-b}{d-c} \text{ [°]} \quad (11)$$

Using equations (3), (4), and (5), the spring stiffness coefficient can be determined:

$$k = \frac{\sin(\arctan\frac{a-b}{d-c}) + \mu\cos(\arctan\frac{a-b}{d-c})}{\Delta x nG\left[\cos(\arctan\frac{a-b}{d-c}) - \mu\sin(\arctan\frac{a-b}{d-c})\right]} \text{ [N/m]} \quad (12)$$

Analysis of the clamping force:

$$\begin{Bmatrix} F_g = G\sin\theta \\ F_z + F_g = F_j \\ F_j = F_f + F_l \\ F_f = \mu_2 F_c \end{Bmatrix} \quad (13)$$

where:

F_g - support force from the branch on the impact clamping device, [N]; F_z - impact force, [N]; F_i - Resultant force of the pre-tension and the pull provided by the Rectangular solenoid, [N]; F_f - Friction force between the Rectangular solenoid and the dynamic clamping head, [N]; μ_2 - static friction coefficient between the Rectangular solenoid and the dynamic clamping head; F_c - magnetic force of the electromagnet, [N].

From equation (9), the required magnetic force of the Rectangular solenoid can be calculated:

$$F_c = \frac{G\sin\theta + F_z - F_l}{\mu_2} \text{ [N]} \quad (14)$$

The higher the harvesting height of the harvester, the stronger the magnetic suction force required to clamp the branches during impact by the exciting electromagnet. Taking the maximum clamping gap and the highest working height as examples, let a =70 mm, b =40mm, c =65mm, d =110 mm, θ=30°, n =0.5. The spring extension deformation corresponds to the clamping diameter of the clamping device, $0 \leqslant \Delta x \leqslant 40$mm.

At this point, Δx =40mm, the spring provides the maximum tensile force, thus meeting the requirements across the entire range. From this, the guide angle is determined to be α =35°, the spring progression coefficient k <376.4N/m, F_c =473N.

Based on the formula for the spring stiffness coefficient:

$$k = \frac{Gd^4}{8D^3n} \text{ [N/m]} \quad (15)$$

From this analysis, the guide angle is determined to be 35°, with the spring progression coefficient being less than 376.4 N/m, and the tensile force provided is 473 N. According to the formula for the spring stiffness coefficient:

RESULTS

Walnut Harvester Picking Trials

During the harvesting process, it is essential to consider how the impact device adapts to walnut branches of varying thicknesses and changes in excitation points. The excitation effect differs significantly depending on the branch diameter: thinner branches show a more pronounced response under excitation, with a wider range and greater efficiency; by contrast, optimizing the harvesting efficiency of thicker branches should be a focal point. Therefore, in order to provide a practical reference for harvesting, this study was planned to conduct multi-point excitation tests on walnut branches of different diameters using different excitation frequencies.

Branches with diameters ranging from 30mm to 56mm and lengths exceeding 2.5m were selected, with data collection facilitated by an in-house developed IM948 sensor module fitted in an electronic walnut. This device utilizes Bluetooth technology to transmit acceleration data to a computer terminal within a frequency range of 0.5-250Hz. The sensor's acceleration component has a range of ±16g, with a minimum change unit accurate to 0.01g. The use of the electronic walnut simulates the acceleration response of the fruit at the end of the branch post-excitation, thus verifying the excitation effects of the harvester and providing a scientific basis for orchard harvesting (see Fig.7).

Fig. 7 - Schematic diagram of the harvesting trials

Trial Strategy and Outcomes

Based on device performance and user experience, branches with diameters of 30mm, 43mm, and 56mm and lengths exceeding 2.5m were selected as test subjects. At positions 800mm, 1200mm, and 1600mm from the main branch, excitation frequencies of 1.67Hz, 2.50Hz, and 3.33Hz were set for testing. During the tests, the electronic walnut mounted on the branches was used to collect dynamic acceleration data of the fruit at the branch ends.

A three-factor, three-level response surface analysis using Design-Expert software was conducted to thoroughly assess the impact of branch diameter, excitation point, and excitation frequency on the excitation effect. The experimental factors and levels are detailed in Table 2, which provides an overview of the comprehensive experimental parameter settings.

Table 2

Table of Trial Factor Levels

Level	Excitation frequency / A	Branch diameter / B	Vibration excitation point / C
	[Hz]	[mm]	[mm]
-1	1.66	30.00	800
0	2.50	43.00	1200
+1	3.33	56.00	1600

The average values of the experimental data for each group were calculated and entered into the experimental design and results table, as shown in Table 3.

Table 3

Trial design and results

Treatment group	excitation frequency / A	branch diameter / B	vibration excitation point / C	vibration acceleration / Y
	[Hz]	[mm]	[mm]	[m/s^2]
1	3.33	56	1200	72
2	2.50	43	1200	93
3	2.50	43	1200	93
4	1.66	56	1200	63
5	1.66	43	800	61
6	1.66	30	1200	110
7	3.33	30	1200	142
8	1.66	43	1600	118
9	2.50	30	800	100
10	2.50	43	1200	93
11	3.33	43	1600	132
12	2.50	56	1600	85
13	2.50	43	1200	93
14	2.50	30	1600	150
15	2.50	56	800	47
16	3.33	43	800	85
17	2.50	43	1200	93

A second-order multivariate regression fit of the data in Table 2 was performed using Design-Expert software, yielding the results of the analysis of variance (ANOVA) for walnut fruit acceleration, as displayed in Table 4.

Tabel 4

Trial ANOVA table

	Sum of Squares	Df	F-value	P-value
Model	12568.51	9	294.00	<0.001**
A	780.13	1	164.24	<0.001**
B	6903.13	1	1453.29	<0.001**
C	4608.00	1	970.11	<0.001**
AB	132.25	1	27.84	0.012*
AC	25.00	1	5.26	0.055
BC	36.00	1	7.58	0.028*
A^2	55.33	1	11.65	0.011*
B^2	0.066	1	0.014	0.909
C^2	23.75	1	5.00	0.060
Residual	33.25	7		
Lack of Fit	33.25	3	0.629	
Pure Error	0	4		
Cor Total	12601.76	16		

Note: "**" indicates highly significant, and "*" indicates significant.

This study conducted a detailed analysis of the acceleration of walnut fruit post-excitation and determined the order of importance of influencing factors based on experimental data. The results indicate that branch diameter, excitation point, and excitation frequency significantly impact acceleration, with the order of influence being: branch diameter > excitation point > excitation frequency. The regression model derived from the analysis is as follows:

$$Y = 92.80 + 9.87A - 29.38B + 24.00C - 75AB - 2.50AC - 3.00BC + 3.72A^2 + 0.22B^2 + 2.48C^2 \quad (17)$$

The model's goodness-of-fit test indicated that the lack-of-fit value was greater than 0.1, confirming the model's high adaptability. The model's high significance was validated with a P-value of 0.0001, and a coefficient of determination (R^2) of 0.9574, indicating that over 95% of the response values can be explained by this model, thus confirming the accuracy of the regression equation in predicting the post-excitation acceleration of walnut fruit.

To further understand the impact of each factor on acceleration, response surface analysis plots for significant interaction factors were generated based on the regression equation, as shown in Fig.8. The analysis revealed:

Optimization of Harvesting Parameters

In the operation of walnut harvesting machines, the excitation effects significantly vary for branches of different diameters, even under the same excitation point and frequency. For thin branches, excessively strong excitation forces may cause branch breakage, while thick branches may require multiple excitations to achieve the desired harvesting effect. To enhance harvesting efficiency and optimize energy utilization, optimization calculations of harvesting parameters were conducted using Design-Expert software, aiming to provide more effective harvesting guidance.

The optimization objective function considered the interactions between excitation force, frequency, and position, with detailed solution analysis conducted through mathematical modeling and constraints (Eq.18).

$$\begin{cases} 100 \le Y \\ 1.6 \le A \le 3.3 \\ 30 \ge B; 30 \le B \le 43; 43 \le B \le 56 \\ 800 \le C \le 2500 \end{cases} \quad (18)$$

The results of the harvesting parameter optimization, as shown in Fig. 9, are as follows:

(a) As the excitation frequency increases, the excitation point required to achieve the necessary acceleration significantly decreases. Therefore, increasing the excitation frequency while ensuring harvesting effectiveness can effectively expand the excitation range. The recommended harvesting parameters are an excitation frequency of 3.33Hz and an excitation point 450mm from the main branch junction.

(b) For branches with diameters ranging from 30mm to 43mm, increasing the excitation point can significantly enhance the excitation effect, while reducing the excitation frequency helps to decrease energy consumption. Therefore, the suggested harvesting parameters are an excitation frequency of 1.66Hz and an excitation point 1400mm from the main branch junction.

(c) For branches with diameters ranging from 43mm to 56mm, the impact of excitation frequency on the excitation effect is minimal, so the frequency can be reduced as much as possible to lower energy consumption. The recommended harvesting parameters are an excitation frequency of 1.66Hz and an excitation point 1800mm from the main branch junction.

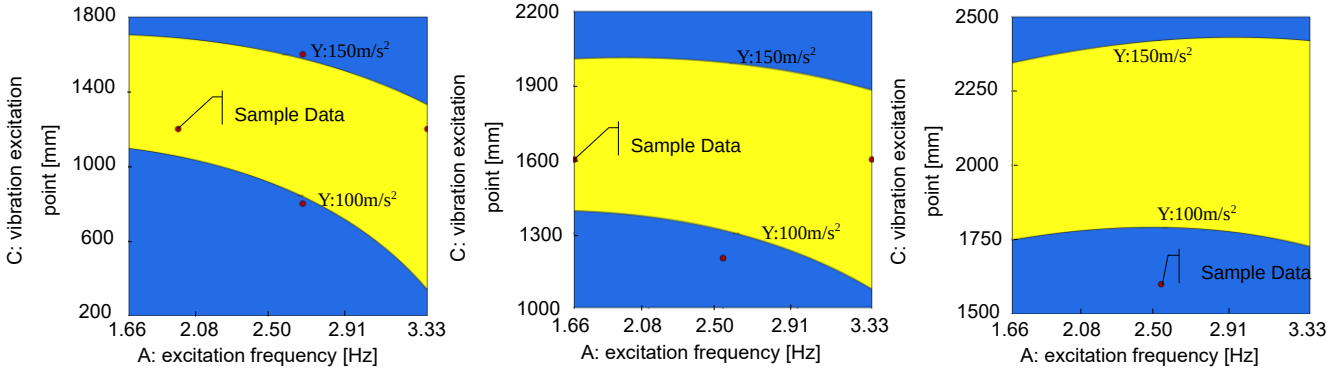

(a) 30≥B (b) 30>B≥43 (c) 43>B≥56

Fig. 9 - Optimization Plot for Harvesting Parameters

CONCLUSIONS

This study successfully designed and experimentally validated a portable walnut harvesting machine tailored for the unique planting patterns of China's hilly regions. The main conclusions and contributions are as follows:

1. The walnut harvester, integrated with an Electric dual-wheel handcart, demonstrated exceptional climbing and obstacle-crossing capabilities, suitable for the complex terrain of hilly areas. Through an adjustable support column and a suspension design, the impact device located at the end of the control rod effectively reduces the transmission of excitation force to the operator while providing flexible control to accommodate various branch growth angles. This significantly improves harvesting efficiency and reduces the labor intensity for farmers.

2. Impact tests indicate that lightweight push plates are less affected by pitch angle and excitation frequency, whereas heavier push plates exhibit greater impact kinetic energy. However, as the pitch angle increases, the impact decreases and the kinetic energy shows a trend of initially increasing then decreasing. Using a push plate made of NM450 material (weight 300g), an impact force of up to 130N was produced at the maximum pitch angle, optimizing the excitation effect.

3. Electronic fruits prepared using the IM948 sensor module were used to collect data, verifying the machine's impact effects under various excitation frequencies, positions, and branch diameters. Experimental results indicated that both the excitation point and branch diameter significantly influence fruit acceleration, with notable effects from excitation frequency as well. Using the Design-Expert software for parameter optimization, the picking parameters for branches of different diameters were optimized. Consequently, for branches with diameters less than 30mm, a recommended excitation frequency of 3.33Hz and an excitation point 450mm from the main branch junction; for branches with diameters of 30 to 43mm, an excitation frequency of 1.66Hz and an excitation point 1400mm from the main branch junction; and for branches with diameters of 43 to 56mm, an excitation frequency of 1.66Hz and an excitation point 1800mm from the main branch junction.

ACKNOWLEDGEMENT

This project is supported by two funding sources. The first one is the National Key Research and Development Program of China, with the project titled "Research and Development of Harvesting Equipment for Walnuts and Goji Berries" (2022YFD2202105).

The second one is the Yunnan Province Rural Revitalization Science and Technology Special Project, titled "Yunnan Province Yangbi County Walnut Industry Science and Technology Special Group" (202204BI090011).

REFERENCES

[1] Castro-Garcia S., Blanco-Roldan G.L., Louise F., Gonzalez-Sanchez E.J., Gil-Ribes J.A., (2017), Frequency response of late-season 'Valencia' orange to selective harvesting by vibration for juice industry. *Biosystems Engineering*, vol.155, pp.77-83, DOI:10.1016/J.BIOSYSTEMSENG.2016.11.012;

[2] Chengmao Cao, Chao Zhan, Yan Sun, Zeze Li, Wentian Wu, Ran Ding., (2018), Design and Experiment of Portable Walnut High-altitude Pat-picking Machine (便携式山核桃高空拍打采摘机设计与试验). *Transactions of the Chinese Society for Agricultural Machinery*, vol.49, no.3, pp.130-137, Beijing/China, DOI: 10.6041/j.issn.1000-1298.2018.03.015;

[3] Chunshou Ye, Kangnni Su, Yuhe Ma, Chenyu Liao, Baoqing Wang, Haifang Hu., (2022), Effect of Walnut-Corn Intercropping on Fruit Quality and Yield of Walnut (核桃-玉米间作对核桃果实品质及产量的影响), *Acta Agriculturae Boreali-occidentalis Sinica*, vol.31, no.10, pp.1365-1373, Shanxi/China, DOI: 10.7606/j.issn.1004-1389.2022.10.013;

[4] Honghong Yu, Ya Li, Lingzhi Liao., (2019), Research on the Development Strategy of Walnut Industry in Yunnan Province (云南省核桃产业发展策略研究), *Problems of Forestry Economy,* vol.39, no.4, pp.427-434, Fujian/China, https://doi.org/10.16832/j.cnki.1005-9709.2019.04.013;

[5] Hoshyarmanesh, H., Dastgerdi, H. R., Ghodsi, M., Khandan, R., Zareinia, K., (2017), Numerical and experimental vibration analysis of olive tree for optimal mechanized harvesting efficiency and productivity, Computers and Electronics in Agriculture, vol.132, pp.34-48, https://doi.org/10.1016/j.compag.2016.11.014;

[6] Huibin Zhu, Wenkai Zhang, Gaocao Ke, Zhenbai Li, Hui Li, Leimu Dan., (2023), Design and Experimental Research on Vibratory Walnut Harvester for Mountainous Areas in Yunnan (云南山地核桃振动采摘机的设计与试验研究), *Journal of Agricultural Mechanization Research*, vol.45, no.2, pp.130-139, Heilongjiang/China, DOI:10.13427/j.cnki.njyi.2023.02.009;

[7] Jia Meng, Xiaopu Fang, Xuanming Shi, Yu Zhang, Jian Liu., (2023), The Current Situation, Problems, and Suggestions for the Development of Walnut Industry in China (我国核桃产业发展现状、问题与建议), *China Lipid*, vol.48, no.1, pp.84-86+103, Shanxi/China, https://doi.org/10.19902/j.cnki.zgyz.1003-7969.220637;

[8] Junming Hou, Yachen Yu, Ziyuan Tang, Liang Zhang, Jiuyu Jin, Wei Wang., (2024), Optimization and experiment on mechanical vibration harvesting process parameters of mulberry, *Journal of INMATEH - Agricultural Engineering* Vol. 72, No. 1 / 2024, DOI: https://doi.org/10.35633/inmateh-72-49;

[9] Mengkun Lu, Junhong Zhang, Xielie Yi, Zhifang Yuan., (2023), Numerical Algorithm of Electromagnetic Force of Cylindrical Push-Pull Electromagnet (圆柱形推拉式电磁铁的电磁力数值算法), *Science Technology and Engineering*, vol.23, no.30, pp.12958-12965, Beijing/China, DOI: 10.3969/j.issn.1671-1815.2023.30.023;

[10] Qiqi Shang, Chengpeng Li, Xiaoning He, Dongwei Wang, Haiqing Wang Shuai Yang., (2023), Design and Experiment of High-acid Apple Vibrating Picker (高酸苹果振动式采摘机设计与试验). *Transactions of the Chinese Society for Agricultural Machinery*, vol.54, no.3, pp.115-125, Beijing/China, DOI:10.6041/j.issn.1000-1298.2023.03.012;

[11] Tong Huang, Baoquan Guo, Tong Zhang, Huping Mao, Ning Ding., (2018). Dynamic characteristics of electromagnetic damper under impact loading (冲击载荷作用下电磁阻尼器动力学特性). *Science Tech nology and Engineering*, vol.18, no.32, pp.174-178, Beijing/China, DOI: 10.3969/j.issn.1671-1815.2018.32.026;

[12] Tuqiang Chen, Guiqing Xu, Jiazhen Chen, Shensi Liu, Jinyao Li, Haifang Hu., (2023), Effects of different water supply amounts on physiology, growth, and fruit quality of walnut trees. (不同灌水量对核桃树生理、生长和果实品质的影响), *Chinese Journal of Ecology*, vol.42, no.11, pp.2578-2587, Beijing/China, Doi: 10.13292/j.1000-4890.202311.016Zicheng Gao, Kaijie Zhao, Lijun Li, Guoyou Pang., (2019), Design and experiment of suspended vibratory actuator for picking Camellia Olerfera fruits (悬挂振动式油茶果采摘执行机构设计与试验). *Transactions of the Chinese Society of Agricultural Engineering (Transactions of the CSAE)*, vol.35, no.21, pp. 9-17, Beijing/China, DOI: 10.11975/j.issn.1002-6819.2019.21.002;

[13] Wei Li., (2023), Analysis and Reflection on the Development Issues of Walnut Industry in China (我国核桃产业发展问题的几点分析与思考), *Northwest Horticulture*, vol.308, no.1, pp.5-7, Shanxi/China , DOI:10.3969/j.issn.1004-4183.2023.02.002;

[14] Wenting Jin, Jinhui Zhao., (2023), Tengfei Zhuang, Zhongjun Liu, Xuejun Yang, Lijing Liu., Review on Theory and Equipment of Mechanical Vibration Picking of Forest Fruits (林果机械振动采摘理论与装备研究进展). *Transactions of the Chinese Society for Agricultural Machinery*, vol.54, no.s1, pp.144-160, Beijing/China, DOI:10.6041/j.issn.1000-1298.2023.S1.016;

[15] Xiaoqiang Du, Chen Ning, Leiyin He, Yin Qian, Guofeng Zhang, Xiaohua Yao., (2022), Design and Test of Crawler-type High Clearance Camellia oleifera Fruit Vibratory Harvester (履带式高地隙油茶果振动采收机设计与试验). *Transactions of the Chinese Society for Agricultural Machinery*, vol.53, no.7, pp.113-121, Beijing/China, DOI:10.6041/j.issn.1000-1298.2022.07.011;

[16] Yi Cao, Zhaodong Wang, Di Wu, Ti Zhang., (2011), Microstructure and mechanical properties of HSLA wear-resistant steel NM400 (NM400 高强度低合金耐磨钢的组织与性能), *Journal of Northeastern University (Natural Science)*, Shenyang/China, vol.32, no.2, pp.241-244;

Zensong Li, Chengmao Cao, Delin Wu, Jianyu Zhang., (2021), Design and experiment of hand-operated self-integrated picking machine for Carya cathayensis (手自一体式山核桃采摘机的设计与试验), *Acta Agriculturae Zhejiangensis*, vol.33, no.7, pp.1309-1319, Zhejiang/China, DOI: 10.3969/j.issn.1004-1524.2021.07.17.